JOURNAL OF BACTERIOLOGY, May 2008, p. 3362–3373 Vol. 190, No. 9
0021-9193/08/$08.00+0 doi:10.1128/JB.02008-07

The *sim* Operon Facilitates the Transport and Metabolism of Sucrose Isomers in *Lactobacillus casei* ATCC 334[▽]

John Thompson,[1]* Nicholas Jakubovics,[2]† Bindu Abraham,[3]¶ Sonja Hess,[3]‡ and Andreas Pikis[1]§

Microbial Biochemistry and Genetics Unit,[1] and Oral Biofilm Communication Unit,[2] Oral Infection and Immunity Branch, NIDCR, and the Proteomics and Mass Spectrometry Facility, NIDDK,[3] National Institutes of Health, DHHS, Bethesda, Maryland 20892

Received 26 December 2007/Accepted 19 February 2008

Inspection of the genome sequence of *Lactobacillus casei* ATCC 334 revealed two operons that might dissimilate the five isomers of sucrose. To test this hypothesis, cells of *L. casei* ATCC 334 were grown in a defined medium supplemented with various sugars, including each of the five isomeric disaccharides. Extracts prepared from cells grown on the sucrose isomers contained high levels of two polypeptides with M_rs of ~50,000 and ~17,500. Neither protein was present in cells grown on glucose, maltose or sucrose. Proteomic, enzymatic, and Western blot analyses identified the ~50-kDa protein as an NAD^+- and metal ion-dependent phospho-α-glucosidase. The oligomeric enzyme was purified, and a catalytic mechanism is proposed. The smaller polypeptide represented an EIIA component of the phosphoenolpyruvate-dependent sugar phosphotransferase system. Phospho-α-glucosidase and EIIA are encoded by genes at the LSEI_0369 (*simA*) and LSEI_0374 (*simF*) loci, respectively, in a block of seven genes comprising the *s*ucrose *i*somer *m*etabolism (*sim*) operon. Northern blot analyses provided evidence that three mRNA transcripts were up-regulated during logarithmic growth of *L. casei* ATCC 334 on sucrose isomers. Internal *simA* and *simF* gene probes hybridized to ~1.5- and ~1.3-kb transcripts, respectively. A 6.8-kb mRNA transcript was detected by both probes, which was indicative of cotranscription of the entire *sim* operon.

Comparative genomics and phylogenetic analyses of the lactic acid bacteria (LAB) have provided evidence that the order *Lactobacillales* comprises the families *Lactobacillaceae*, *Streptococcaceae*, *Enterococcaceae*, and *Leuconostocaceae* (17, 25; http://www.ncbi.nlm.nih.gov/Taxonomy/). These generally fastidious gram-positive organisms are used extensively for the fermentation of dairy, meat, and vegetable products. The industrial importance of LAB, and *Lactobacillus casei* strains in particular, results from the capacity of these microorganisms to metabolize carbohydrates rapidly (and primarily) to lactic acid. Prior to their homolactic fermentation via the glycolytic pathway, many carbohydrates are accumulated simultaneously with phosphorylation via sugar-specific phosphoenolpyruvate (PEP)-dependent phosphotransferase systems (PTSs) (7, 24, 29). The multicomponent PEP-dependent PTSs comprise membrane-localized, sugar-specific transporters (IICB enzymes) that may be fused or associated with a third protein (EIIA), as well as two general cytoplasmic proteins (EI and HPr). Collectively, these interactive proteins constitute a five-stage phosphorelay that, via transfer of the high-energy phosphoryl moiety from PEP, catalyzes the simultaneous phosphorylation and translocation of sugars through the cytoplasmic membrane. Biochemical and physiological studies performed during the past 25 years have established the presence of a variety of sugar PEP-dependent PTSs in *L. casei*, including PTSs for glucose (41, 45), galactose (2, 6), lactose (4, 5, 8, 9), sorbose (46), and pentitols (15, 16). Significantly, in the past decade, the development and application of techniques for manipulation of LAB genomes have provided extensive (and in some instances unexpected) insight into the molecular basis for regulation of PEP-dependent PTSs in *L. casei* (18, 42, 45).

Many bacterial species, including *L. casei*, have the capacity to transport sucrose via an inducible sucrose-specific PEP-dependent PTS (GenBank accession no. YP_807293). Intracellular sucrose-6-phosphate is subsequently hydrolyzed to glucose-6-phosphate (G6P) and fructose by sucrose-6-phosphate hydrolase (GenBank accession no. YP_807296). The latter cofactor-independent 6-phosphoglucosyl hydrolase has been assigned to family 32 of the 110-member glycosyl hydrolase (GH) superfamily (11, 12; Carbohydrate-Active Enzyme Database [http://www.cazy.org/fam/acc_GH.html]). In contrast to the commonly observed dissimilation of sucrose, it was assumed for a long time that microorganisms are unable to metabolize the five linkage-isomeric α-D-glucosyl-D-fructose isomers of sucrose, namely, trehalulose, turanose, maltulose, leucrose, and palatinose. However, studies in our laboratory have proved that this assumption is invalid by showing that several species belonging to both gram-positive and gram-negative genera readily utilize these isomeric disaccharides as energy sources for growth (23, 30, 34, 36, 37). Remarkably, besides the five sucrose isomers, these organisms also transport a variety of related O-α-linked glycosides, including maltose, isomaltose, maltitol, and α-methyl-D-glucoside, by the α-glucoside-specific PEP-dependent PTS. Furthermore, the accumulated α-glu-

* Corresponding author. Mailing address: Microbial Biochemistry and Genetics Unit, NIDCR, National Institutes of Health, Bldg. 30, Rm. 325, Convent Dr. MSC-4350, Bethesda, MD 20892. Phone: (301) 496-4083. Fax: (301) 402-1064. E-mail: jthompson@dir.nidcr.nih.gov.

† Present address: School of Dental Sciences, Newcastle University, Framlington Place, Newcastle upon Tyne NE2 4BW, England.

¶ Center for Biologics Evaluation and Research, Food and Drug Administration, Bethesda, MD 20892.

‡ Proteome Exploration Laboratory, California Institute of Technology, Pasadena, CA 91125.

§ Center for Drug Evaluation and Research, Food and Drug Administration, Silver Spring, MD 20993.

▽ Published ahead of print on 29 February 2008.

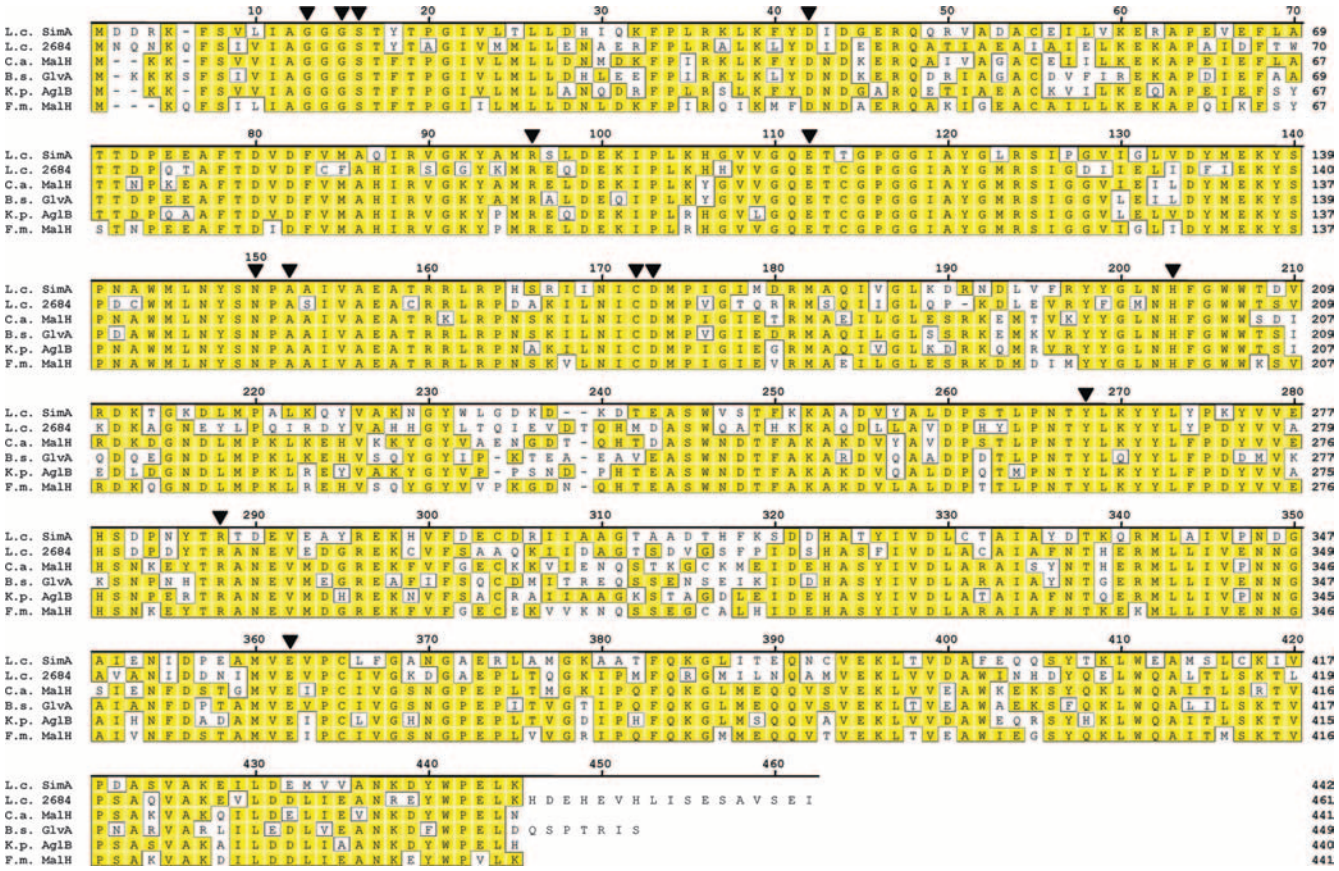

FIG. 1. Comparative sequence alignment of NAD^+- and metal ion-dependent Pagls belonging to the GH4 family. Genes in *L. casei* ATCC 334 are numbered in accordance with the annotation in the GenBank database (accession no. NC_008526). The sequences of the following proteins are shown: putative Pagls encoded by *L. casei* ATCC 334 LSEI_0369 (*simA*) (accession no. YP_805670) (L.c. SimA) and LSEI_2684 (YP_807845) (L.c. 2684) and enzymes purified from *C. acetobutylicum* (Swiss-Prot accession no. Q97LM4) (C.a. MalH), *B. subtilis* (accession no. P54716) (B.s. GlvA), *K. pneumoniae* (accession no. Q9AGA7) (K.p. AglB), and *F. mortiferum* (accession no. O06901) (F.m. MalH). The numbers on the right indicate the numbers of amino acids per protein, and conserved amino acids are highlighted. The filled triangles indicate (*L. casei simA* numbering) residues that comprise the NAD^+-binding domain of the βαβ Rossmann fold (residues 6 to 72; importantly, G12, G14, S15, and D41), proton donor residue D172, proton acceptor residue Y265, residues that coordinate with the Mn^{2+} ion (including A151, C171, and H202), and amino acids that participate in substrate binding (including R95, N149, and R285). Residue E111 increases the basicity of the catalytically essential residue Y265 (28).

coside-6-phosphates are hydrolyzed by a novel NAD^+- and Mn^{2+}-dependent phospho-α-glucosidase (Pagl) (EC 3.2.1.122) that is assigned to the unique GH family 4 (GH4) (3, 14, 27, 34, 36, 39).

Thus far, there have been no reports of the utilization of sucrose isomers by representatives of the families *Streptococcaceae* and *Lactobacillaceae*, including the species residing in plaque (at the tooth surface) or in biofilms in the oral cavity (20, 21). Consequently, these "noncariogenic" and comparatively sweet disaccharides are used increasingly as substitutes for dietary sucrose (10). Our interest in this area of carbohydrate dissimilation by LAB stemmed from in silico mining of data in the recently published genome sequence of *L. casei* strain ATCC 334 (GenBank accession no. NC_008526). Inspection of this chromosomal DNA sequence revealed two putative PTS operons (see Fig. 2A and B) that have genes at the LSEI_2684 and LSEI_0369 loci. The deduced amino acid sequences encoded by the two genes showed unusually high levels of identity with the NAD^+- and Mn^{2+}-dependent Pagls described previously for other bacteria. From the comparative alignments shown in Fig. 1, we hypothesized that expression of the products of one (or both) of these operons might also facilitate growth of *L. casei* ATCC 334 on sucrose isomers, maltose, and related α-linked glucosides. A collaborative study was initiated to test this hypothesis, and our findings are presented in this paper.

MATERIALS AND METHODS

Materials. High-purity sugars, including glucose, sucrose [α-D-glucopyranosyl-β-D-fructofuranoside, α(1→2) linkage], maltose (4-*O*-α-D-glucopyranosyl-D-glucopyranose), and 1-*O*-methyl-α-D-glucopyranoside, were purchased from Pfanstiehl Laboratories, Inc. Maltitol (4-*O*-α-glucopyranosyl-D-sorbitol), chromogenic *p*-nitrophenyl-α-D-glucopyranosides, and isomaltose (6-*O*-α-D-glucopyranosyl-D-glucose) were obtained from Sigma and TCI America. The five linkage isomers of sucrose were obtained from the following sources: trehalulose (α, 1→1) was a generous gift from Südzucker, Germany; turanose (α, 1→3) was obtained from Pfanstiehl; maltulose (α, 1→4) was obtained from TCI America; leucrose (α, 1→5) was obtained from Fluka; and palatinose (α, 1→6) was purchased from Wako Chemicals. Phosphorylated derivatives, including

trehalulose-6′-phosphate, sucrose-6-phosphate, turanose-6′-phosphate, maltulose-6′-phosphate, leucrose-6′-phosphate, palatinose-6′-phosphate, maltose-6′-phosphate, isomaltose-6′-phosphate, and maltitol-6-phosphate, were prepared enzymatically (38). Chromogenic phosphate derivatives, including *p*-nitrophenyl-α-glucopyranoside-6-phosphate (pNPαG6P), were prepared by selective phosphorylation with phosphorus oxychloride in trimethyl phosphate containing small proportions of water (33). Phosphorylated β-linked disaccharides, including 4-*O*-β-D-glucopyranosyl-D-glucopyranoside-6′-phosphate (cellobiose-6′-phosphate) and 6-*O*-β-D-glucopyranosyl-D-glucopyranose-6′-phosphate (gentiobiose-6′-phosphate), were prepared by phosphorylation of the parent compounds with purified ATP-dependent β-glucoside kinase (EC 2.7.1.85) from *Klebsiella pneumoniae* (35). $NADP^+$, Ultrogel AcA-44, Tris-Acryl M-DEAE, and other materials were supplied by Sigma-Aldrich. Glucose-6-phosphate dehydrogenase (G6PDH) (EC 1.1.1.49) was obtained from Roche Molecular Biochemicals.

Organism, maintenance, and growth medium. *L. casei* ATCC 334 was obtained from the American Type Culture Collection (Manassas, VA) and was maintained in MRS broth (Difco) supplemented with 0.2% (wt/vol) glucose. The medium used for growth of *L. casei* ATCC 334 contained (per liter) 10 g Trypticase (BBL), 0.5 g yeast extract (Difco), 3 g tryptone peptone (Difco), 3 g KH_2PO_4, 3 g K_2HPO_4, 1.7 g sodium acetate · $3H_2O$, 1.2 g sodium citrate · $2H_2O$, and 1 ml Tween 80. Prior to autoclaving, the pH of the medium was adjusted to 7 by addition of 5 N NaOH. After this, 100 ml of a filter-sterilized salts solution was prepared, which contained 11.6 g $MgSO_4 \cdot 7H_2O$, 2.4 g $MnSO_4 \cdot 2H_2O$, and 0.6 g $FeSO_4 \cdot 7H_2O$. Prior to inoculation, 5 ml $liter^{-1}$ of the salts solution was added to the medium, and filter-sterilized sugar solutions were added to obtain a final concentration of 0.4% (wt/vol). Organisms were grown to stationary phase in 1-liter capped bottles at 37°C (in the absence of a fermentable carbohydrate, there is not significant growth of *L. casei* ATCC 334 in this medium).

Analytical methods. The molecular weight of denatured PagI (subunit) was determined by sodium dodecyl sulfate (SDS)-polyacrylamide gel electrophoresis (PAGE) using the Novex XCell mini-cell system (Invitrogen). Novex NuPage (4 to 12% acrylamide) bis-Tris gels and morpholineethanesulfonic acid (MES)-SDS running buffer (pH 7.3) were used together with Novex Mark12 protein standards. Polypeptides were visualized by staining with Coomassie blue R-250. For Western blots, proteins and SeeBlue-prestained standards were transferred to nitrocellulose membranes using NuPage transfer buffer. Immunodetection of PagI was performed by sequential incubation of the membrane with (i) polyclonal antibody to PagI (MalH) (EC 3.2.1.122) from *Fusobacterium mortiferum* and (ii) goat anti-rabbit horseradish peroxidase-conjugated antibody as described previously (33). The native molecular weight of PagI was determined by gel filtration on the same AcA-44 column used for purification. The column was calibrated with the following standards: alcohol dehydrogenase (150 kDa), bovine serum albumin (66 kDa), ovalbumin (43 kDa), and chymotrypsinogen A (25 kDa). Protein concentrations of cell extracts were determined with a BCA assay kit (Pierce Chemical Co.). The N-terminal sequence of PagI was determined with an ABI 477A protein sequencer (Applied Biosystems Inc.) with an online ABI 120A phenylthiohydantoin analyzer. Two-dimensional (2D) PAGE for proteomic analyses was carried out by Kendrick Laboratories, Inc., and protein spots (see Fig. 4A and B) were identified by matrix-assisted laser desorption ionization–time of flight mass spectrometry (Applied Biosystems Voyager DE Pro instrument) by M. A. Gawinowicz, Protein Core Facility, Columbia University, New York, NY.

For identification of major proteins (see Fig. 4, spots 1 to 23), the Coomassie blue-stained spots were excised and destained prior to reduction with dithiothreitol, alkylation with iodoacetamide, and digestion with trypsin. Tryptic peptides were reconstituted in formic acid (6.4 μl, 0.1% [vol/vol]) and concentrated on a C_{18} Optipak (Bodman Industries) trap column. After a 10-min delay, the sample was directed to a Vydac C_{18} column (100 mm by 150 μm [inside diameter]; 5 μm; Microtech Scientific) for separation. Solvent A was a mixture of 98.8% water, 1% acetonitrile, and 0.1% formic acid, and solvent B was a mixture of 98.8% acetonitrile, 1% water, and 0.1% formic acid. The gradient was increased from 5% solvent B to 95% solvent B in 40 min at a flow rate of 50 $\mu l\ min^{-1}$ and was split at a 10:1 ratio on the column. The eluent from the liquid chromatography system was introduced into a linear ion trap Fourier transform ion cyclotron mass spectrometer (Thermo Electron, San Jose, CA) by electrospray ionization. The following instrument settings were used: source voltage, 3.05 kV; capillary voltage, 40.00 V; tube lens voltage, 80.00 V; and capillary temperature, 200°C. Tryptic fragments were generated by collision-induced dissociation at a normalized collision energy of 35% and an activation Q of 0.250. Tandem mass spectrometry (MS-MS) data were acquired with the Xcalibur 2.0 software and processed using Bioworks to create data (dta) files. These files were merged to obtain mfg files suitable for database searching using the MASCOT database search engine (www.matrixscience.com). The following parameters were used: database, SPTREMBLE; taxonomy, *Firmicutes* (gram-positive bacteria); one missed cut cleavage; iodoacetamidation of cysteines; and charge states of +2, +3, and +4. A window of 10 ppm for mass accuracy for precursor ions and 0.6-Da mass accuracy for MS-MS data was chosen. The results were parsed on Scaffold (Proteome Software, Portland, OR). Only proteins that were identified by at least two peptides and >95% peptide probability (based on MASCOT and Protein Prophet scores) were chosen.

Assay of PagI activity. The activity of the NAD^+- and Mn^{2+}-dependent PagI in cell extracts and during purification was measured colorimetrically with pNPαG6P as the substrate. Enzyme activity was determined using a discontinuous assay and a mixture that contained (in 2 ml) Tris-HCl buffer (50 mM, pH 7.5), $MnCl_2$ (1 mM), NAD^+ (1 mM), and pNPαG6P (0.5 mM). After equilibration at 37°C, the reactions were initiated by addition of an enzyme preparation. Samples (0.25 ml) were removed at 20-s intervals and immediately injected into 0.75 ml of a 0.5 M Na_2CO_3 solution containing 0.1 M EDTA to stop the reaction. The absorbance at 400 nm was measured, and the rates of *p*-nitrophenol formation were calculated from progress plots, assuming that the molar extinction coefficient (ε) at pH 10.2 for the yellow *p*-nitrophenolate anion was 18,300 $M^{-1}\ cm^{-1}$. PagI activity was expressed in nanomoles (or micromoles) of *p*-nitrophenol formed per minute per milligram of protein. A continuous spectrophotometric method was used to measure the rates of hydrolysis of α-glucoside-6-phosphate substrates. This G6PDH/$NADP^+$-coupled assay monitored the release of G6P in a 1-ml reaction mixture that contained Tris-HCl buffer (0.1 M, pH 7.5), $MnCl_2$ (1 mM), $MgCl_2$ (1 mM), NAD^+ (1 mM), $NADP^+$ (1 mM), substrate (1 mM), and ~3 U of G6PDH. Reactions were started by adding the enzyme preparation, and the increase in A_{340} was monitored with a Beckman DU 640 recording spectrophotometer. The initial rates of G6P formation were calculated using the kinetics program of the instrument. A molar extinction coefficient (ε) of 6,220 $M^{-1}\ cm^{-1}$ was assumed for calculation of the amount of NADPH formed (amount of G6P released). PagI activity was expressed in nanomoles of phosphorylated substrate hydrolyzed per minute per milligram of protein.

Cloning and expression of the *L. casei* ATCC 334 PagI gene (*simA*) in *Escherichia coli* TOP10. Based on the complete genome sequence of *L. casei* ATCC 334, the following pair of primers was designed to amplify the *simA* gene: forward primer 5′-GGGCCCC**ATGGATGATCGGAAGTTTTCAGTTTTAATTG**C-3′ (the *simA* sequence is in boldface type, and the NcoI restriction site is underlined) and reverse primer 5′-CGAGCAGAATTC**CTACTTCAGTTCTGG CCAGTAGTC**-3′ (the sequence complementary to the downstream region of *simA* is in boldface type, and the EcoRI restriction site is underlined). PCR amplification was carried out with a thermal cycler (GeneAmp 9700PCR system; PE Applied Biosystems) using *Pfu* high-fidelity DNA polymerase from Stratagene. The components of the amplification mixture (100 μl) were as follows: 5 U of *Pfu* DNA polymerase, 1× reaction buffer provided by the manufacturer, 20 mM each of the four deoxynucleoside triphosphates, 250 ng of each primer, 100 ng of *L. casei* ATCC 334 chromosomal DNA, and 1% (vol/vol) dimethyl sulfoxide. After an initial 2-min incubation at 95°C, the mixture was subjected to 30 cycles of amplification under the following conditions: denaturation at 95°C for 1 min, annealing at 50°C for 1 min, and extension at 72°C for 2 min/kb of insert. This procedure was followed by a 10-min runoff at 72°C. The amplicon was digested with restriction endonucleases NcoI and EcoRI, electrophoresed in a 1% agarose gel, and purified (QIAquick gel extraction kit). The purified ~1.3-kbp PCR product was ligated to similarly digested and purified expression vector pTrcHis2B (Invitrogen) to form the recombinant plasmid pTrcHis2B*simA* (designated pAP*simA*). In this construct, the *simA* gene is under control of the *trc* promoter. Since pTrcHis vectors also contain a copy of the *lacI*^{q} gene, expression of the *simA* gene is fully induced in the presence of isopropyl-β-D-thiogalactopyranoside (IPTG). Recombinant plasmid pAP*simA* was transformed into *E. coli* TOP10 (Invitrogen) competent cells, and colonies were selected on Luria-Bertani (32) agar plates containing 150 $\mu g\ ml^{-1}$ ampicillin. It should be noted that in the pTrcHis2B vector the fusion peptide is located at the C terminus rather than the N terminus, as is the case for pTrcHis vectors. However, the stop codon included in our reverse primer prevented the expression of the fusion peptide in the pTrcHis2B vector.

Purification of PagI from *E. coli* TOP10(pAP*simA*). The plasmid-containing cells were grown in 800 ml Luria-Bertani broth containing ampicillin (150 $\mu g\ ml^{-1}$) in 2-liter baffled flasks at 37°C on a rotary shaker at 200 rpm. At an A_{600} of 0.4 to 0.6 U, IPTG (0.5 mM) was added to each culture, and the culture was grown for 3 h. The culture was harvested by centrifugation (13,000 × *g* for 10 min at 5°C), and the cells (2.4 g $liter^{-1}$) were washed by resuspension and centrifugation from Tris-HCl buffer (25 mM, pH 7.5) containing $MnCl_2$ (1 mM), NAD^+ (0.1 mM), and dithiothreitol (1 mM) (TMND buffer).

(i) Preparation of cell extract. Washed cells (18 g, wet weight) were resuspended in 45 ml of TMND buffer, and the organisms were disrupted (at 0°C) by

1.5 min of sonic oscillation twice using a Branson instrument (model 350) operating at ~75% of the maximum power. The extract was clarified by two centrifugations; the first centrifugation was a low-speed centrifugation (25,000 × *g* for 30 min at 5°C) and was followed by ultracentrifugation at 180, 000 × *g* for 2 h at 5°C. The high-speed supernatant was transferred to sacs and dialyzed in a cold room for 16 h against 4 liters of TMND buffer. Pagl was purified to homogeneity by a simple two-stage chromatographic procedure.

(ii) Step 1: Tris-Acryl M-DEAE anion exchange. Dialyzed high-speed supernatant (56 ml) was transferred at a flow rate of 0.5 ml min^{-1} to a column of Tris-Acryl M-DEAE (2.6 by 15 cm) previously equilibrated with TMND buffer containing dithiothreitol (5 mM). Nonadsorbed material was removed by passage of this buffer through the column. After this, Pagl was eluted with 500 ml of a linear increasing-concentration gradient of NaCl (0 to 0.4 M) in TMND buffer. Fractions (5 ml) were collected, and Pagl activity was detected by the intense yellow color formed upon addition of fraction samples (10 μl) to microtiter wells containing 100 μl of pNPαG6P assay solution. The fractions with the greatest activity (fractions 52 to 60) were pooled and concentrated to 6.5 ml by pressure filtration (50 lb/in^2) through an Amicon PM-10 membrane.

(iii) Step 2: Ultrogel AcA gel filtration. Approximately 2 ml of DEAE concentrate was applied at a flow rate of 0.15 ml min^{-1} to a column of Ultrogel AcA-44 (1.6 by 94 cm) previously equilibrated with TMND buffer containing 0.1 M NaCl. Fractions (2 ml) were collected, and the fractions containing the maximum Pagl activity (fractions 49 to 55) were pooled. This procedure was twice repeated with the remaining two 2-ml portions of DEAE concentrate. The appropriate fractions (fractions 49 to 55) from each of the three runs were pooled and concentrated with an Amicon pressure cell to a final volume of 10 ml. Assuming that the M_r of the Pagl monomer was 49,711 and that the extinction coefficient (ε) was 73,145 M^{-1} cm^{-1}, the concentration of highly purified Pagl in the sample was calculated to be 13.9 mg ml^{-1} and the specific activity was calculated to be 3.78 μmol of pNPαG6P hydrolyzed min^{-1} mg $protein^{-1}$.

Extraction of RNA from *L. casei* ATCC 334. Total RNA was extracted from exponential-phase cells (optical density at 600 nm, ~0.8) cultured in medium containing glucose, sucrose, or sucrose isomers as the sole energy source. Two volumes of RNAprotect (Qiagen) was added to 1 volume of cells, and samples were mixed and then incubated at 25°C for 5 min. Cells were harvested by centrifugation at 3,500 × *g* at 25°C for 15 min, and following removal of the supernatant by aspiration, cells were stored at −70°C for 24 h. Cell pellets were thawed, resuspended in 1 ml Trizol reagent (Invitrogen), and transferred to FastPrep blue tubes containing lysing matrix B (Qbiogene). Cells were mechanically disrupted with a FastPrep bead beater (Qbiogene) for 40 s at speed setting 6 and allowed to stand at 25°C for 10 min. Chloroform (0.2 ml) was added, and samples were mixed and incubated for 3 min at 25°C. Following centrifugation at 12,000 × *g* for 15 min, the aqueous phase was collected and mixed with 0.5 ml isopropanol to precipitate RNA. Samples were incubated at 25°C for 10 min, and RNA precipitates were recovered by centrifugation at 12,000 × *g* for 10 min. Pellets were washed twice in 75% (vol/vol) ethanol and air dried. Purified RNA was dissolved in 50 μl H_2O and stored at −70°C.

Northern blot procedures. Expression of specific transcripts was assessed by Northern blotting using a NorthernMax kit (Ambion) according to the manufacturer's instructions. Briefly, RNA was thawed on ice, and 5 μg of each RNA sample was subjected to electrophoresis through a 1% (wt/vol) agarose gel. RNA was transferred to a BrightStar Plus membrane (Ambion) under a vacuum pressure of 5 mm Hg for 1.5 h in a model 785 vacuum blotter (Bio-Rad). Membranes were fixed using a Stratalink UV cross-linker (Stratagene) and prehybridized for 30 min at 42°C in ULTRAhyb buffer (Ambion). Oligonucleotide DNA probes internal to the *simA* (5′-GCAAAGACTCATCGCTTCCCAAAGTTTGGTGTACGATTGC-3′) and *simF* (5′-CGAGTGGCATAAGGATGCCCGTGACAGGGGCAATAATCGGCTGTCC-3′) genes were synthesized and 5′ end labeled with ^{32}P (Lofstrand Labs). Following prehybridization, probes were added at a final concentration of 10^6 cpm ml^{-1} and incubated for 16 h at 42°C. Membranes were washed twice at 25°C for 5 min in low-stringency wash solution no. 1 (Ambion) and once at 42°C in high-stringency wash solution no. 1. Washed membranes were exposed to Kodak BioMax MR film for 10 h.

Sequence alignment and operon prediction. Protein sequences were aligned by using the Clustal W algorithm in the MegAlign software (DNASTAR Inc.). The structure of operons was predicted by automated genome annotation using the fgenesB module of the MolQuest software (Softberry Inc.). Putative promoter and terminator elements were identified as part of the annotation pipeline. A potential catabolite response element (CRE box) was found in the promoter region of *simA* by using the Virtual Footprint software program (http://prodoric.tu-bs.de/vfp/) to search the *simABCDEFG* operon and upstream sequence for close matches to a position weight matrix based on the CRE box elements upstream of 13 *Bacillus subtilis* genes.

RESULTS

Identification of putative α-glucoside PTS operons in *L. casei* ATCC 334. A BLAST search (1) of the *L. casei* ATCC 334 genome with the gene encoding the NAD^+- and Mn^{2+}-dependent Pagl (GlvA) of *B. subtilis* as the probe revealed two sequences encoding proteins with strikingly high homology to this enzyme. The LSEI_2684 gene encodes a 461-amino-acid protein that exhibits 60% identity with GlvA, whereas LSEI_0369 (*simA*) encodes a smaller protein (442 residues) with 62% sequence identity with GlvA. The translation products of the two *L. casei* genes, which exhibit 59% sequence identity (Fig. 1), were also remarkably similar to the sequences of Pagls recently purified from *Fusobacterium mortiferum* (MalH) (3), *K. pneumoniae* (AglB) (37), and *Clostridium acetobutylicum* (MalH) (34). These NAD^+- and Mn^{2+}-requiring enzymes are assigned to the unique GH4 family of the GH superfamily, and the comparative sequence alignment of the six proteins revealed strict conservation of the 14 active site residues known to participate in binding of the nucleotide, metal ion, and substrate during catalysis (28, 34, 36).

To identify genes that might be cotranscribed with LSEI_2684 or LSEI_0369 and might be subject to similar transcriptional regulation, the genome of *L. casei* ATCC 334 was scanned for predicted promoters and terminators using automated annotation software (Fig. 2). No promoter was identified immediately upstream of LSEI_2684, and the gene was predicted to be cotranscribed with LSEI_2685, which encodes EIICA components of the PTS (Fig. 2A). In the *L. casei* genome annotation, LSEI_2685 is designated a pseudogene because it contains a frameshift mutation that likely causes premature truncation during translation. A σ^{70} consensus promoter was identified in the upstream noncoding region of LSEI_0369, and a Rho-independent transcription terminator was predicted downstream of the LSEI_0369 stop codon (Fig. 2B). No other consensus promoter was located in the sequence containing LSEI_0369 to LSEI_0373. Therefore, expression of LSEI_0370 to LSEI_0373 requires either an atypical promoter element or transcription readthrough from LSEI_0369. A σ^{70}-type promoter was predicted upstream of LSEI_0374, and a characteristic Rho-independent transcription terminator was identified downstream of LSEI_0375. The putative proteins encoded by LSEI_0370 to LSEI_0375 inclusive are shown in Fig. 2B. A CRE box sequence was identified between the −10 promoter element and the ATG start codon of LSEI_0369, suggesting that this promoter may be under carbon catabolite (CcpA) control. Upstream of LSEI_0369 there was an open reading frame (LSEI_0368) that was predicted to encode a transcriptional regulator. From these in silico analyses, we hypothesized that the operon shown in Fig. 2B might facilitate growth of *L. casei* ATCC 334 on α-glucoside substrates, including the isomers of sucrose. For convenience, genes in this multicistronic operon were designated *sim* (*s*ucrose *i*somer *m*etabolism) genes.

Pagl activity in cell extracts of *L. casei* ATCC 334. *L. casei* ATCC 334 grew readily on the 12 sugars tested, including all five isomers of sucrose (Table 1). Cell extracts were prepared, and the Pagl activity of these extracts was assayed using chromogenic pNPαG6P as the substrate. Comparatively high levels of enzyme activity were found in organisms grown previously

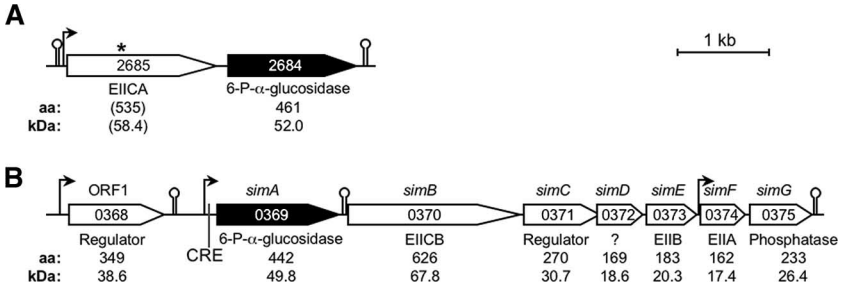

FIG. 2. Gene organization of the two operons which encode the putative NAD^+- and Mn^{2+}-dependent PagIs in *L. casei* ATCC 334. The predicted function, amino acid (aa) chain length, and protein molecular mass are indicated under each gene. Potential promoters (bent arrows) and terminators (lollipop symbols) were predicted in silico. (A) Operon A. The LSEI_2684 gene encoding a putative Pagl is predicted to be transcribed from a promoter upstream of LSEI_2685. In the National Center for Biotechnology Information database (http://www.ncbi.nlm.nih.gov) LSEI_2685 is annotated as a pseudogene. The asterisk indicates a frameshift mutation that may prevent expression of the EII(CA) component of the PTS. (B) Operon B hypothesized to participate in sucrose isomer metabolism (*sim*). The LSEI_0369 (*simA*), LSEI_0370 (*simB*), and LSEI_0374 (*simF*) genes putatively encode a Pagl, a membrane-localized PTS transporter complex [EII(CB)], and an intracellular EIIA component of the PTS, respectively.

on the α-glucosides described above, whereas little or no Pagl activity was detectable in extracts of cells grown previously on glucose, sucrose, melezitose, or maltose (the significance of the latter result is described in the Discussion). SDS-PAGE analysis revealed high levels of expression of a ~50-kDa protein in the extracts that contained Pagl activity (Fig. 3A) and that cross-reacted strongly with polyclonal antibody against purified Pagl (MalH) from *F. mortiferum* (Fig. 3B).

Proteomic analyses. Because of the similarities in the theoretical masses of the proteins encoded by LSEI_0369 (M_r, 48,842) and LSEI_2684 (M_r, 52,030), neither the results of the enzymatic analyses nor the results of Western blotting permitted differentiation between the putative Pagl enzymes. To differentiate these enzymes, proteomic analyses of cell extracts were performed by using 2D PAGE (Fig. 4). Because the Pagl expression was minimal in glucose- or sucrose-grown organisms, the proteomic profiles of these extracts served as references for comparison with protein expression in cells grown on four sucrose isomers. The results of 2D PAGE revealed gen-

TABLE 1. Pagl activity in extracts prepared from cells of *L. casei* 334 grown on various sugars

Sugar in growth medium[a]	Pagl activity (nmol pNPαG6P hydrolyzed min^{-1} mg $protein^{-1}$)[b]
Glucose	~0.4
Methyl-α-D-glucopyranoside	22.6
Melezitose	NDA[c]
Trehalose	NDA
Maltose	NDA
Isomaltose	15.8
Sucrose	NDA
Trehalulose[d]	15.8
Turanose[d]	2.1
Maltulose[d]	10.0
Leucrose[d]	15.0
Palatinose[d]	15.2

[a] Organisms were grown in a medium containing individual sugars at a final concentration of 0.4% (wt/vol).
[b] The values are averages of at least two determinations, and the variation was 5 to 10%.
[c] NDA, no detectable activity.
[d] The compound is an isomer of sucrose.

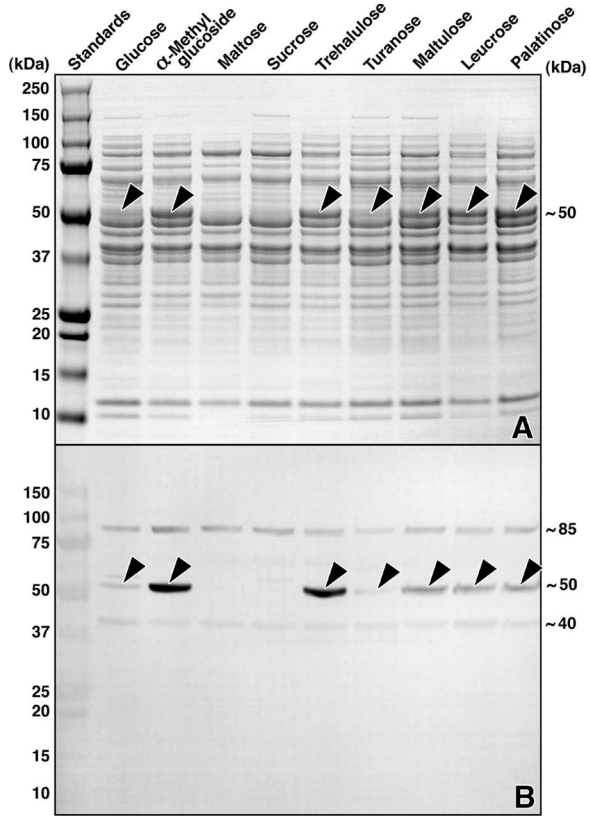

FIG. 3. SDS-PAGE and Western blot analyses of extracts from cells of *L. casei* ATCC 334 grown on various sugars. (A) SDS-PAGE and visualization of proteins by Coomassie blue R-250 staining. Approximately 30 μg protein was applied per lane. Note the expression (arrowheads) of a ~50-kDa protein induced by growth on the five sucrose isomers. This polypeptide is either absent or barely detectable in similarly prepared extracts from organisms grown previously on glucose, sucrose, or maltose. (B) Western blot of a duplicate gel, showing the cross-reactivity of the induced protein (arrowheads) with polyclonal antibody raised against the NAD^+- and Mn^{2+}-dependent Pagl (MalH) from *F. mortiferum*. The identities of the ~40 and ~85-kDa immunoreactive polypeptides are unknown.

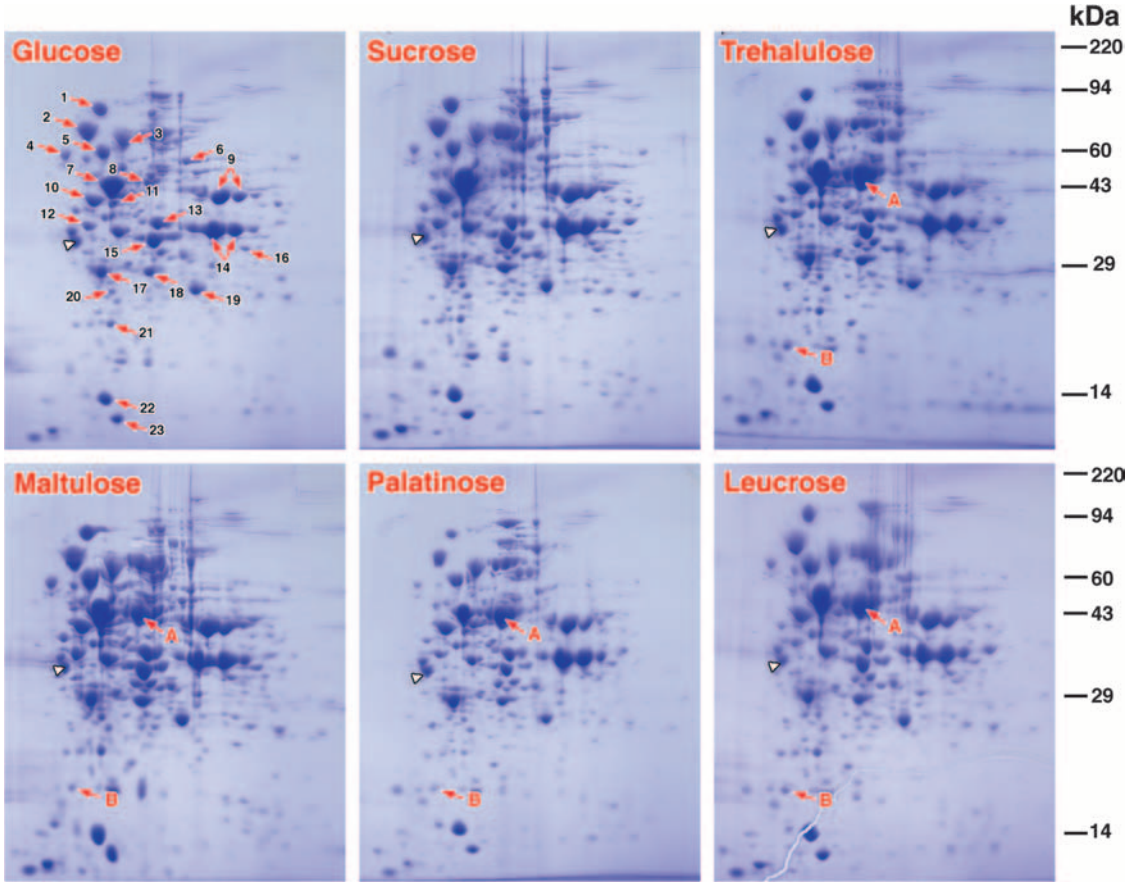

FIG. 4. Proteomic analyses by 2D PAGE of extracts of *L. casei* ATCC 334 cells grown separately on glucose, sucrose, and four isomers of sucrose. 2D electrophoresis revealed a remarkable similarity in the polypeptide composition, and 23 highly conserved proteins were identified by MS-MS in all extracts (Table 2). However, extracts prepared from cells grown on the four sucrose isomers contained high levels of two proteins (spots A and B) that were not detected in extracts from either glucose- or sucrose-grown cells. The identities of the two "spots" were determined after excision, tryptic digestion, and MS-MS. The extensive peptide coverage established that proteins A (M_r, ~50,000) and B (M_r, ~17,000) were encoded by LSEI_0369 (*simA*) and LSEI_0374 (*simF*), respectively, of operon B (Fig. 2). The arrowhead indicates the position of the internal standard tropomyosin (32.7 kDa; pI 5.2) included in each of the gels. The molecular weight standards used were myosin (220,000), phosphorylase A (94,000), catalase (60,000), actin (43,000), carbonic anhydrase (29,000), and lysozyme (14,000).

erally similar proteomic profiles, and 23 common proteins were readily identified in all cell extracts (Table 2). However, two polypeptides, polypeptides A (M_r, ~50,000) and B (M_r, ~17,000), were present in the proteome of cells grown on the sucrose isomers. Neither protein was detectable in extracts from glucose- or sucrose-grown organisms. For identification, spots A and B were excised from the gels and treated with trypsin, and peptide fragments in the digests were characterized by liquid chromatography–MS-MS. Peptides identified in the digest of spot A accounted for 77% of the predicted sequence of the PagI encoded by LSEI_0369 (*simA*) of the operon (Fig. 2B). Peptides recovered from the digest of spot B comprised 92% of the amino acid sequence deduced by translation of LSEI_0374 (*simF*), confirming that polypeptide B was the EIIA component of an α-glucoside PEP-dependent PTS. In the NCBI database, the accession number of the phosphoglycosyl hydrolase (442 residues; M_r, 49,842) is YP_805670, and the accession number of the EIIA protein (162 amino acids; M_r, 17,351) is YP_805674.

Expression, purification, and properties of PagI (*simA*). The procedures used for expression and purification of PagI from the transformant *E. coli* TOP10(pAP*simA*) are described in Materials and Methods. The four-step purification procedure yielded 140 mg of PagI (specific activity, 3.78 μmol of pNPαG6P hydrolyzed min^{-1} mg $protein^{-1}$), and SDS-PAGE of the denatured enzyme revealed a single polypeptide with an M_r of ~50,000 (Fig. 5A). The homogeneity of the preparation was confirmed by unambiguous determination of the first 30 residues from the N terminus by microsequence analysis: MD DRKFSVLIAGGGSTYTPGIVLTLLDHIQ. This sequence is the same as the sequence deduced by translation of the PagI gene (*simA*). The molecular weights of PagI determined from two electrospray ionization-mass spectrometry measurements (48,837 and 49,851) compared favorably with the theoretical average molecular weight (49,842) deduced from the amino acid sequence encoded by *simA*. However, passage of the native protein through a calibrated gel filtration column (AcA-44; exclusion limit, ~200 kDa) yielded an M_r of 95,000 to 120,000

TABLE 2. Identification by MS-MS of prominent proteins present in all cell extracts of *L. casei* 334 revealed by 2D PAGE (Fig. 4)

Spot	Protein	Accession no.	Mol wt (10^3)	pI
1	Translation elongation factor (GTPase)	YP_807686	76.7	4.77
2	Chaperone protein (HSP70)	YP_806781	67.4	4.77
3	PTS enzyme I (EC 2.7.3.9)	YP_806973	63.3	5.00
4	Pyruvate kinase (EC 2.7.1.40)	YP_806585	62.7	5.20
5	Chaperonin GroEL (HSP 60)	YP_807425	57.4	4.89
6	AICAR transformylase (EC 2.1.2.3)	YP_806961	54.7	5.40
7	GTPase elongation factor(s)	YP_806555	43.4	4.87
8	Oxaloacetate decarboxylase (EC 4.1.1.3)	YP_807056	51.8	5.10
9	3-Phosphoglycerate kinase (EC 2.7.2.3)	YP_806208	42.1	5.64
10	Enolase (EC 4.2.1.11)	YP_806210	47.0	4.73
11	DNA polymerase/clamp unit (EC 2.7.7.7)	YP_805310	41.3	4.64
12	Elongation factor fragment	YP_805520	40.1	4.84
13	Tagatose-1,6-bisphosphate aldolase (EC 4.1.2.40)	YP_807760	36.2	5.25
14	Glyceraldehyde-3-phosphate dehydrogenase (EC 1.2.1.12)	YP_806207	36.6	5.68
15	L-Lactate dehydrogenase (EC 1.1.1.27)	YP_807714	35.4	5.24
	Catabolite control protein (CcpA)	YP_806087	36.3	5.26
16	UDP-glucose-4-epimerase (EC 5.1.3.2)	YP_805947	36.2	5.69
17	Triose phosphate isomerase (EC 5.3.1.1)	YP_806209	26.8	4.87
18	dTDP-glucose pyrophosphorylase (EC 2.7.7.24)	YP_807212	32.2	5.48
19	Phosphoglycerate mutase (EC 5.4.2.1)	YP_807326	25.8	5.43
20	DNA-binding protein (Ssb)	YP_805318	21.0	5.14
21	ATP-dependent Clp protease fragment/subunit	YP_806204	21.4	5.09
22	PTS phosphocarrier protein (HPr)	YP_806974	9.1	4.91
23	Chaperonin GroES (Cpn 10)	YP_807426	9.9	4.93

for Pagl. Furthermore, the results obtained from cross-linking experiments with homobifunctional imidoesters provided evidence of formation of a dimeric protein that was a similar size (~100 kDa), as well as trimeric and tetrameric oligomers (Fig. 5B). It is likely that in solution Pagl exists primarily in the homodimeric form, but our data do not preclude the possibility that there is a mixture of catalytically active dimer and tetramer species.

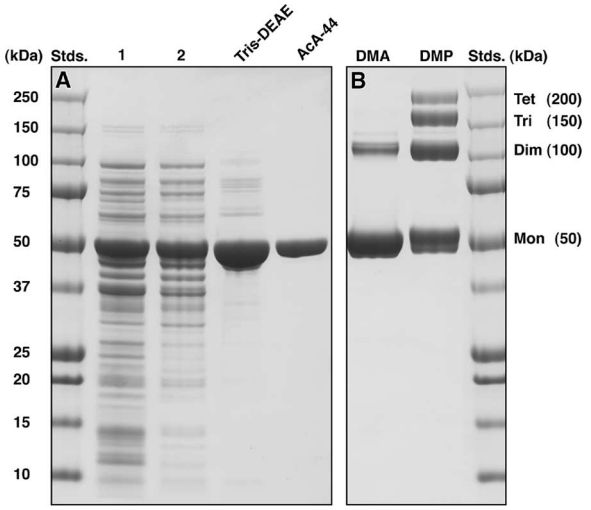

FIG. 5. (A) SDS-PAGE of samples from each of the four stages of the Pagl purification procedure. TMND buffer was used throughout the purification. The chromogenic analog pNPαG6P was used as the substrate for the assay of Pagl activity. Analysis of purified Pagl by SDS-PAGE revealed a single polypeptide at an M_r of ~50,000 (lane AcA-44). (B) Cross-linking of the ~50-kDa subunits of Pagl in the presence of the homobifunctional imidoesters dimethyl adipimidate (lane DMA) and dimethyl pimelimidate (lane DMP) revealed formation of dimeric, trimeric, and tetrameric forms of the enzyme. Whether these oligomeric species exhibit catalytic activity is unknown. Stds., standards.

Cofactor requirements and substrate specificity of Pagl. The GH4 family comprises a variety of hydrolases, including 6-phospho-α-glucosidases, 6-phospho-β-glucosidases, α-glucosidases, and α-galactosidases (http://www.cazy.org). All members of this unique family require a nucleotide (NAD^+), a divalent metal ion, and usually reducing conditions for optimum activity. Table 3 shows that Pagl from *L. casei* ATCC 334 is also dependent on the same cofactors for hydrolysis of pNPαG6P. The importance of a metal ion (e.g., Mn^{2+}) in

TABLE 3. Cofactor requirements for activity of purified Pagl from *L. casei* 334

Addition(s) to basal assay mixture[a]	Pagl activity (μmol pNPαG6P hydrolyzed min^{-1} mg $protein^{-1}$)[b]
None	0.22 ± 0.04
NAD^+	0.72 ± 0.12
Mn^{2+}	1.74 ± 0.15
$NAD^+ + Mn^{2+}$	2.68 ± 0.25
$NAD^+ + Mn^{2+}$ + EDTA (5 mM)	NDA[c]
$NAD^+ + Co^{2+}$	2.32 ± 0.18
$NAD^+ + Ni^{2+}$	2.23 ± 0.23
$NAD^+ + Fe^{2+}$	2.16 ± 0.11
$NAD^+ + Mg^{2+}$	1.33 ± 0.09
$NAD^+ + Zn^{2+}$	NDA

[a] The basal assay mixture (2 ml) contained 50 mM Tris-HCl buffer (pH 7.5) and 0.5 mM pNPαG6P. Cofactors were included at a final concentration of 1 mM. After 3 min of incubation at 37°C, the reaction was initiated by addition of 5 μl (69.5 μg) of purified enzyme that previously had been dialyzed for 16 h at 4°C against 25 mM Tris-HCl buffer (pH 7.5). Substrate hydrolysis was monitored as described in Materials and Methods.

[b] The values are averages ± standard deviations of at least three independent measurements.

[c] NDA, no detectable activity.

TABLE 4. Substrate specificity of purified Pagl from *L. casei* 334[a]

Substrate[b]	Rate of substrate hydrolysis[c]
Trehalulose-6′-phosphate (α, 1-1$_f$)[d]	267
Sucrose-6-phosphate (α, 1-2$_f$)	NDA[e]
Turanose-6′-phosphate (α, 1-3$_f$)[d]	135
Maltulose-6′-phosphate (α, 1-4$_f$)[d]	411
Leucrose-6′-phosphate (α, 1-5$_f$)[d]	62
Palatinose-6′-phosphate (α, 1-6$_f$)[d]	256
Maltose-6′-phosphate (α, 1-4$_g$)	54
Trehalose-6-phosphate (α, 1-1$_g$)	6
Methyl-α-G6P	298
Methyl-β-G6P	NDA
Cellobiose-6′-phosphate (β, 1-4$_g$)	NDA
Gentiobiose-6′-phosphate (β, 1-6$_g$)	NDA
Cellobiitol-6-phosphate (β)	NDA
pNPαG6P	3.78
p-Nitrophenyl-α-galactopyranoside-6-phosphate	NDA
p-Nitrophenyl-α-mannopyranoside-6-phosphate	NDA

[a] The $NADP^+$/G6PDH-coupled spectrophotometric assay used with sugar 6-phosphate derivatives and the chromogenic assay employed with phosphorylated *p*-nitrophenyl substrates are described in Materials and Methods.

[b] The substrates were added to all reaction mixtures at a final concentration of 1 mM.

[c] The rates of hydrolysis of phosphorylated sugars are expressed in nanomoles of G6P formed per minute per milligram of protein. The rates of hydrolysis of chromogenic (*p*-nitrophenyl) substrates are expressed in micromoles of *p*-nitrophenol formed per minute per milligram protein. The rates are the means of three separate determinations.

[d] The compound is an isomer of sucrose.

[e] NDA, no detectable activity.

catalysis is evident from the complete loss of Pagl activity when a chelating agent (EDTA) is added to the reaction mixture. α-Glucosides transported via the PEP-dependent PTS are accumulated as phosphorylated derivatives, and to verify the function of Pagl, it was necessary to demonstrate the enzyme-catalyzed cleavage of these compounds. Investigation of the substrate specificity of Pagl was possible because of our previous syntheses of a variety of phosphorylated disaccharides with both α and β conformations (35, 38). Consistent with its purported physiological role, Pagl hydrolyzed all phosphorylated α-glucosides tested, including the five isomeric derivatives of sucrose (Table 4). Importantly, neither sucrose-6-phosphate nor O-β-linked phosphorylated conformers were hydrolyzed by the enzyme. Experiments conducted with the three chromogenic compounds revealed the requirement for equatorial orientation of the OH groups at C-2 and C-4 of the G6P moiety for cleavage of the glycosidic linkage. Whereas pNPαG6P was readily hydrolyzed by Pagl, neither the C-2 nor the C-4 axial OH isomer (*p*-nitrophenyl-α-mannopyranoside-6-phosphate and *p*-nitrophenyl-α-galactopyranoside-6-phosphate, respectively) was a substrate for the enzyme.

Northern blot analysis of the *sim* operon. To study regulation of the *sim* operon, RNA was extracted from exponential-phase cells of *L. casei* ATCC 334 cultured with glucose, sucrose, or a sucrose isomer as the sole energy source, and the RNA was analyzed by Northern hybridization with *simA*- or *simF*-specific probes (Fig. 6). No *simA* mRNA was detected in RNA preparations from glucose- or sucrose-grown cells. However, a strong band at ~1.5 kb, the predicted size of a monocistronic *simA* transcript, was observed in extracts from cells cultured on maltulose, leucrose, and palatinose (Fig. 6). A band at ~6.8 kb was also detected in these samples and likely corresponded to a seven-gene *simABCDEFG* transcript. The 6.8-kb band was also observed in preparations from sucrose isomer-grown cells by hybridization with the *simF* probe. Additionally, a ~1.3-kb band, corresponding to a bicistronic *simFG* transcript, was detected with the *simF* probe. This transcript was not present in RNA from cells cultured with glucose or sucrose and thus appeared to be under regulation similar to that of *simA* transcripts. The Northern blot data, together with a transcriptional map of the *sim* operon, are shown in Fig. 7.

DISCUSSION

Recent publications have described the growth of several species of bacteria (*K. pneumoniae*, *F. mortiferum*, *B. subtilis*, and *C. acetobutylicum*) on O-α-linked glucosides. However, to our knowledge, this is the first report of the metabolism of the five isomers of sucrose by an LAB. Physiological, biochemical, and genetic evidence supports our hypothesis that expression of proteins encoded by a seven-gene (*sim*) operon (Fig. 2B) facilitates the transport, phosphorylation, and hydrolysis of sucrose isomers (but not sucrose per se) by *L. casei* ATCC 334. By contrast, the functions of polypeptides encoded by the two genes of a smaller operon (Fig. 2A) are unknown, and we obtained no evidence of their expression in our studies. Because of a midgene frameshift, the putative EII(CA) transporter is unlikely to be functional, and while the LSEI_2684 gene almost certainly encodes an NAD^+- and metal-dependent Pagl, the properties and substrate specificity of this GH4 enzyme cannot be determined until it is expressed and purified.

Catalytic mechanism of Pagl from *L. casei* ATCC 334. Many disaccharide phosphate hydrolases have been characterized (43, 44), including 6-phospho-β-galactosidase (EC 3.2.1.85), 6-phospho-β-glucosidase (EC 3.2.1.86), and sucrose-6-phosphate hydrolase (EC 3.2.1.26). These hydrolases do not require cofactors for activity, and on the basis of primary sequence alignment, the first two enzymes are assigned to family 1 and

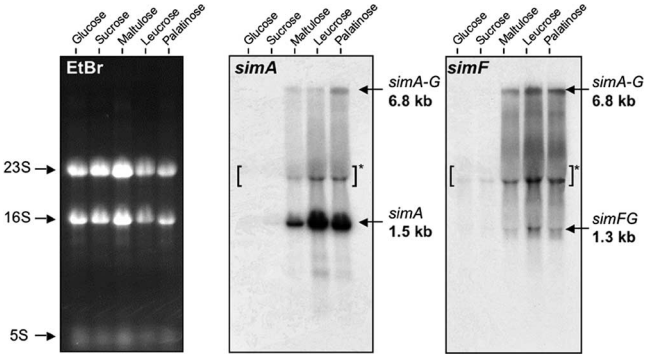

FIG. 6. Northern blot analyses of the *sim* operon. Total RNA was extracted from cells of *L. casei* ATCC 334 growing exponentially on the five sugars indicated. Hybridizations were performed using ^{32}P-labeled probes corresponding to internal DNA regions of *simA* and *simF*. A 6.8-kb mRNA transcript was detected by both probes, which was indicative of cotranscription of all seven genes of the *sim* operon during growth on three sucrose isomers. The *simA* and *simF* probes also hybridized with 1.5- and 1.3-kb transcripts, respectively. The apparent band at ~3 kb (brackets and asterisk) is a commonly observed compression artifact caused by the 23S rRNA. Ethidium bromide (EtBr)-stained rRNAs (23S, 16S, and 5S) served as loading controls (left blot).

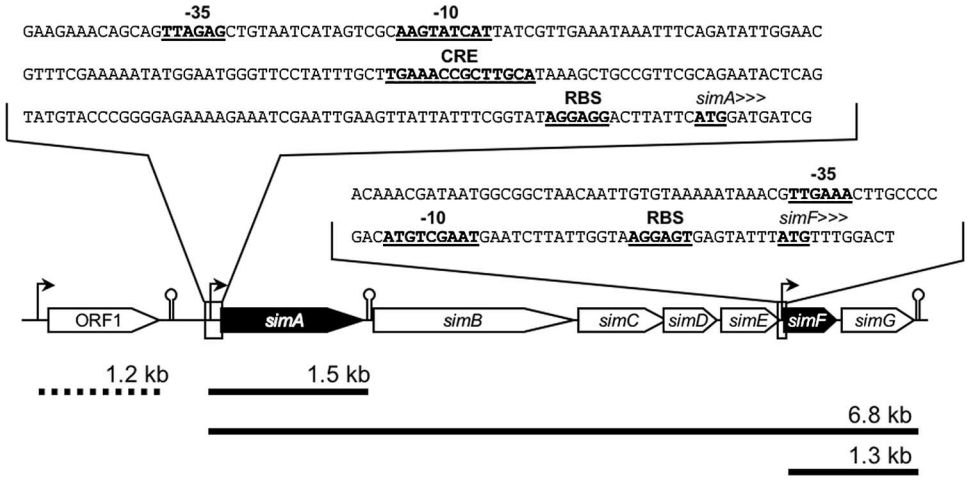

FIG. 7. Map of the *sim* operon, showing the promoter regions of *simA* and *simF*. The −35 and −10 boxes of potential promoters, the translational start codons, the putative CRE site, and the ribosomal binding sites (RBS) are indicated by boldface type and underlining. The heavy solid lines indicate RNA transcripts found only in *L. casei* ATCC 334 cells grown on the isomers of sucrose. The heavy dashed line indicates the ORF1 transcript.

the third enzyme is assigned to family 32 of the GH superfamily. In a landmark article in 1953, Koshland formulated two classic mechanisms for glycoside hydrolysis (13). These mechanisms have withstood the test of time and have received copious support from structural and mechanistic analyses of enzymes throughout the 109 members of the GH superfamily (31, 50, 51). In Koshland's scheme, two acidic residues (Glu and Asp) acting as a general acid or base catalyze hydrolysis of the glycosidic linkage such that (i) the reaction product has an anomeric configuration opposite that of the substrate (direct displacement or inversion) or (ii) the reaction product maintains the same C-1 configuration as the substrate (double displacement or retention).

The requirements of family GH4 enzymes (including PagI from *L. casei* ATCC 334) for NAD^+ and a divalent metal ion are unprecedented for glycosidases, but for some time it was not clear whether these two cofactors play structural and/or catalytic roles in enzyme activity (14, 26, 27, 36, 39). The requirement for NAD^+ suggested that there is a redox step in the hydrolytic process, a possibility inconsistent with either of Koshland's general mechanisms. Equally perplexing was the finding that the dinucleotide cofactor was not consumed during hydrolysis, and no NADH was formed at the end of the catalytic cycle. It was only in 2004, after the solution of the structures of the first GH4 PagI (GlvA from *B. subtilis*; Protein Data Bank code 1u8x) and phospho-β-glucosidase (BglT from *Thermotoga maritima*; Protein Data Bank code 1up6) and extensive kinetic analyses, that a catalytic mechanism could be proposed for these unique enzymes (28, 40, 47–49). In this mechanism, hydrolysis proceeds via a sequence of oxidation-elimination-addition and reduction reactions, which result in overall retention of the configuration at the anomeric center. Figure 1 shows that the 14 catalytically functional residues of GlvA are strictly conserved in PagI, and it is reasonable to assume that there is a similar six-step mechanism for cleavage of the phosphorylated isomers of sucrose by the *L. casei* enzyme (Fig. 8). We believe that in the initial oxidative step, PagI catalyzes the extraction of the hydride from C-3 by NAD^+, yielding enzyme-bound NADH. The attendant base-catalyzed deprotonation of the C-3 OH group (possibly effected by a metal-bound hydroxide) forms a ketone at the C-3 position of the G6P moiety. Ketone formation causes acidification of the C-2 proton and its subsequent removal by a suitably situated base, Tyr 265. Proton extraction at C-2 is also facilitated by the Mn^{2+} ion, which polarizes the carbonyl at C-3 and stabilizes the resultant enolate species. Cleavage of the anomeric C-1—*O*-fructose bond by acid-catalyzed assistance from Asp 172 causes the elimination of the fructose moiety of the disaccharide and formation of an enzyme-bound α,β-unsaturated ketone intermediate. A water molecule is then added to the anomeric center of this unsaturated Michael acceptor, and reprotonation at C-2 is catalyzed by Tyr 265 via reversal of the abstraction process. In the final step, the C-3 keto intermediate is reduced by the "on-board" NADH to form G6P. The reaction cycle, resulting in the production of G6P and fructose from the sucrose-6-phosphate isomer, is now complete, and PagI assumes its original NAD^+-activated state.

Genetic composition and regulation of the *sim* operon in *L. casei* ATCC 334. The α-glucoside PEP-dependent PTS operons of *F. nucleatum* (3, 23), *K. pneumoniae* (37, 38), *B. subtilis* (36), and *C. acetobutylicum* (34) consist of only three genes that encode a transcriptional regulatory protein (RpiR/GntR), an NAD^+- and Mn^{2+}-dependent PagI (designated MalH, AglB, or GlvA), and a membrane-localized EII(CB) transporter of the PTS. It is noteworthy that all of these operons lack a gene encoding EIIA, the small intracellular phosphotransfer protein that is a prerequisite for complementation and functional activity of the PTS. Previously, we hypothesized that an EIIA component from a separate PTS must substitute for the "missing" protein in the species mentioned above (23, 34). This hypothesis was tested and verified by the finding that plasmid-mediated transfer and expression of the *aglA* [EII(CB)] and *aglB* (PagI) genes from *K. pneumoniae* to *E. coli* K-12 conferred upon the latter strain the capacity to metabolize a wide variety of α-glucosides provided that the *E. coli* strain contained a functional $EIIA^{glc}$ of the glucose PTS (22).

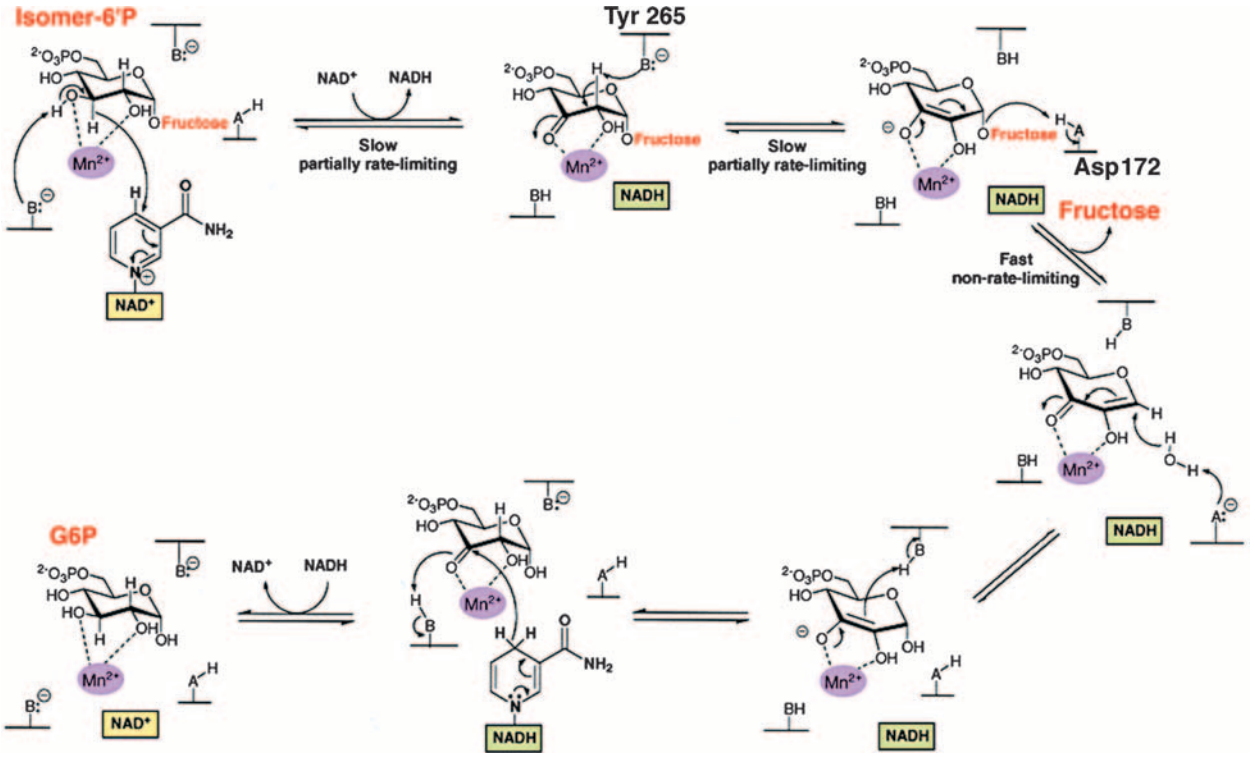

FIG. 8. Proposed mechanism for the hydrolysis of phosphorylated isomers of sucrose by the NAD^+- and Mn^{2+}-dependent PagI from *L. casei* ATCC 334. (Adapted from reference 47 with permission of the publisher.)

By contrast, the *sim* operon of *L. casei* ATCC 334 comprises seven genes, one of which (*simF*) encodes an EIIA protein of the PTS. The fact that this EIIA protein is expressed during growth on the isomers of sucrose suggests that the ~17-kDa polypeptide plays an important and perhaps essential role in α-glucoside PEP-dependent PTS activity in *L. casei* ATCC 334. Details of the mechanism(s) for the regulation of expression of the *sim* operon have not been elucidated yet, but two findings are of interest. First, typical −35 and −10 promoter regions, a ribosome binding site, and a sequence consisting of 14 nucleotides that exhibit the consensus of a CRE occur immediately upstream of the first gene (*simA*) of the operon (Fig. 7). Second, results from Northern blot experiments revealed an mRNA fragment whose size (6.8 kb) is consistent with transcription of the entire seven-gene operon during growth of *L. casei* ATCC 334 on sucrose isomers (Fig. 6 and 7). These results, together with the lack of transcription during growth on rapidly metabolized substrates (glucose and sucrose), suggest that regulation of the *sim* operon is mediated via carbon catabolite repression. This mode of regulation of catabolic operons, particularly those involved in the dissimilation of sugars, is found in many species of gram-positive bacteria, including strains of *L. casei* (7, 18, 41, 45). It is likely that the CRE region is the target for a multicomponent complex (phosphorylated disaccharide, catabolite control protein A [CcpA], and phospho-seryl-HPr) that modulates expression of the *sim* operon in *L. casei* ATCC 334.

Metabolism of maltose by *L. casei* ATCC 334. The α-glucoside PEP-dependent PTS operon that facilitates the metabolism of sucrose isomers in *F. mortiferum*, *K. pneumoniae*, *B. subtilis*, and *C. acetobutylicum* is also induced by, and allows the dissimilation of, maltose in these bacteria. Surprisingly, this is not the case in *L. casei* ATCC 334, and cells grown on the α(1→4)-linked diglucoside contain neither the NAD^+- and Mn^{2+}-dependent PagI nor the EIIA protein encoded in the *sim* operon (Table 1 and Fig. 3).

There must be an alternate route for transport and catabolism of maltose in *L. casei*, and in recent reports Monedero et al. (18, 19) showed that the dissimilation of maltose in *L. casei* strain BL23 is facilitated by the products encoded by two non-PTS *mal* operons. The larger operon (*mal1*) comprises 10 genes, which are directionally opposed to a smaller five-gene operon (*mal2*). The first gene in the *mal1* operon (*malR*) encodes a transcriptional regulator, and this gene is followed sequentially by *malL*, *nplT*, *mapA*, *pgmA*, *malK1*, *dexB*, *malE1*, *malF1*, and *malG1*. Comparative genomic analyses also revealed the presence of *mal2* in the *L. casei* ATCC 334 strain used by Monedero et al. However, in the *mal1* operon of this strain there is a 52-bp deletion in *nplT* (pseudogene LSEI_0981), and a 6.3-kb excision caused the loss of *dexB*, *malE1*, *malF1*, *malG1*, and a portion of the *malK1* gene. Because of these extensive deletions, the strain of *L. casei* ATCC 334 used by Monedero et al. (in contrast to our strain) is unable to grow on maltose. Clarification of these conflicting observations and of other questions pertaining to the regulation of maltose metabolism in *L. casei* strains must await future investigations.

Summary: sucrose metabolism and etiology of dental caries. For numerous reasons, sucrose is a "problem child" in oral biology. For example, this disaccharide provides the molecular

precursors for the synthesis of a glycan(s) that facilitates adherence of streptococci to the tooth surface. The subsequent fermentation of sucrose to lactic acid causes the localized demineralization of tooth enamel and initiation of dental caries. Prior to our studies, it was generally assumed that oral microorganisms (including mutans streptococci and lactobacilli) are unable to metabolize the isomers of sucrose. The fact that these isomeric compounds are comparatively sweet and are produced on an industrial scale has encouraged the use of these purportedly "noncariogenic" disaccharides as substitutes for sucrose in various food products. The genes required for the utilization of sucrose isomers are not present in the genome of *Streptococcus mutans*, but whether oral strains of lactobacilli can metabolize these compounds has yet to be determined. *L. casei* ATCC 334 is used extensively in the dairy industry as a starter for cheese manufacture and is not a common resident of the oral microflora. However, in view of the potential for interspecies transfer of genetic material, we wonder if the widespread use of sucrose isomers will "encourage" dissimilation of this metabolic trait in oral bacteria. Selection of extant lactobacilli or of new species capable of utilizing the isomers of sucrose could conceivably change the composition and metabolic activities of oral biofilms.

ACKNOWLEDGMENTS

We thank Rick Dreyfuss for assistance with photography and computer graphics, Nga Nguyen for microsequence analyses, and Mary Ann Gawinowicz for mass spectrometry fingerprinting. Experiments by Sonja Hess and Bindu Abraham were conducted at the Proteomics and Mass Spectrometry Facility of NIDDK.

This work was supported by the Intramural Research Programs of the NIDCR and NIDDK, National Institutes of Health, Bethesda, MD.

REFERENCES

1. **Altschul, S. F., T. L. Madden, A. A. Schäffer, J. Zhang, Z. Zhang, W. Miller, and D. J. Lipman.** 1997. Gapped BLAST and PSI-BLAST: a new generation of protein database search programs. Nucleic Acids Res. **25:**3389–3402.
2. **Bettenbrock, K., U. Siebers, P. Ehrenreich, and C.-A. Alpert.** 1999. *Lactobacillus casei* 64H contains a phosphoenolpyruvate-dependent phosphotransferase system for uptake of galactose, as confirmed by analysis of *ptsH* and different *gal* mutants. J. Bacteriol. **181:**225–230.
3. **Bouma, C. L., J. Reizer, A. Reizer, S. A. Robrish, and J. Thompson.** 1997. 6-Phospho-α-D-glucosidase from *Fusobacterium mortiferum*: cloning, expression, and assignment to family 4 of the glycosylhydrolases. J. Bacteriol. **179:**4129–4137.
4. **Chassy, B. M., and C.-A. Alpert.** 1989. Molecular characterization of the plasmid-encoded lactose-PTS of *Lactobacillus casei*. FEMS Microbiol. Rev. **63:**157–165.
5. **Chassy, B. M., and J. Thompson.** 1983. Regulation of lactose-phosphoenolpyruvate dependent phosphotransferase system and β-D-phosphogalactoside galactohydrolase activities in *Lactobacillus casei*. J. Bacteriol. **154:**1195–1203.
6. **Chassy, B. M., and J. Thompson.** 1983. Regulation and characterization of the galactose-phosphoenolpyruvate-dependent phosphotransferase system in *Lactobacillus casei*. J. Bacteriol. **154:**1204–1214.
7. **Deutscher, J., C. Francke, and P. W. Postma.** 2006. How phosphotransferase system-related protein phosphorylation regulates carbohydrate metabolism in bacteria. Microbiol. Mol. Biol. Rev. **70:**939–1031.
8. **Gosalbes, M. J., V. Monedero, C.-A Alpert, and G. Pérez-Martínez.** 1997. Establishing a model to study the regulation of the lactose operon in *Lactobacillus casei*. FEMS Microbiol. Lett. **148:**83–89.
9. **Gosalbes, M. J., V. Monedero, and G. Pérez-Martínez.** 1999. Elements involved in catabolite repression and substrate induction of the lactose operon in *Lactobacillus casei*. J. Bacteriol. **181:**3928–3934.
10. **Hamada, S.** 2002. Role of sweeteners in the etiology and prevention of dental caries. Pure Appl. Chem. **74:**1293–1300.
11. **Henrissat, B., and A. Bairoch.** 1996. Updating the sequence-based classification of glycosyl hydrolases. Biochem. J. **316:**695–696.
12. **Henrissat, B., and G. Davies.** 1997. Structural and sequence-based classification of glycoside hydrolases. Curr. Opin. Struct. Biol. **7:**637–644.
13. **Koshland, D. E., Jr.** 1953. Stereochemistry and the mechanism of enzymatic reactions. Biol. Rev. **28:**416–436.
14. **Lodge, J. A., T. Maier, W. Liebl, V. Hoffmann, and N. Sträter.** 2003. Crystal structure of *Thermotoga maritima* α-glucosidase AglA defines a new clan of NAD^+-dependent glycosidases. J. Biol. Chem. **278:**19151–19158.
15. **London, J., and N. M. Chace.** 1979. Pentitol metabolism in *Lactobacillus casei*. J. Bacteriol. **140:**949–954.
16. **London, J., and S. Z. Hausman.** 1983. Purification and characterization of the III^{Xtl} phospho-carrier protein of the phosphoenolpyruvate-dependent xylitol:phosphotransferase found in *Lactobacillus casei* Cl83. J. Bacteriol. **156:**611–619.
17. **Makarova, K., A. Slesarev, Y. Wolf, A. Sorokin, B. Mirkin, E. Koonin, A. Pavlov, N. Pavlova, V. Karamychev, N. Polouchine, V. Shakhova, I. Grigoriev, Y. Lou, D. Rohksar, S. Lucas, K. Huang, D. M. Goodstein, T. Hawkins, V. Plengvidhya, D. Welker, J. Hughes, Y. Goh, A. Benson, K. Baldwin, J.-H. Lee, I. Diaz-Muniz, B. Dosti, V. Smeianov, W. Wechter, R. Barabote, G. Lorca, E. Altermann, R. Barrangou, B. Ganesan, Y. Xie, H. Rawsthorne, D. Tamir, C. Parker, F. Breidt, J. Broadbent, R. Hutkins, D. O'Sullivan, J. Steele, G. Unlu, M. Saier, T. Klaenhammer, P. Richardson, S. Kozyavkin, B. Weimer, and D. Mills.** 2006. Comparative genomics of the lactic acid bacteria. Proc. Natl. Acad. Sci. USA **103:**15611–15616.
18. **Monedero, V., A. Mazé, G. Boël, M. Zuniga, S. Beaufils, A. Hartke, and J. Deutscher.** 2007. The phosphotransferase system of *Lactobacillus casei*: regulation of carbon metabolism and connection to cold shock response. J. Mol. Microbiol. Biotechnol. **12:**20–32.
19. **Monedero, V., M. J. Yebra, S. Poncet, and J. Deutscher.** 4 November 2007, posting date. Maltose transport in *Lactobacillus casei* and its regulation by inducer exclusion. Res. Microbiol. doi:10.1016/j.resmic.2007.10.002.
20. **Ooshima, T., A. Izumitani, S. Sobue, N. Okahashi, and S. Hamada.** 1983. Non-cariogenicity of the disaccharide palatinose in experimental dental caries of rats. Infect. Immun. **39:**43–49.
21. **Ooshima, T., A. Izumitani, T. Minami, T. Fujiwara, Y. Nakajima, and S. Hamada.** 1991. Trehalulose does not induce dental caries in rats infected with mutans streptococci. Caries Res. **25:**277–282.
22. **Pikis, A., S. Hess, I. Arnold, B. Erni, and J. Thompson.** 2006. Genetic requirements for growth of *Escherichia coli* K12 on methyl-α-D-glucopyranoside and the five α-D-glucosyl-D-fructose isomers of sucrose. J. Biol. Chem. **281:**17900–17908.
23. **Pikis, A., S. Immel, S. A. Robrish, and J. Thompson.** 2002. Metabolism of sucrose and its five isomers by *Fusobacterium mortiferum*. Microbiology **148:**843–852.
24. **Postma, P. W., J. W. Lengeler, and G. R. Jacobson.** 1993. Phosphoenolpyruvate:carbohydrate phosphotransferase systems of bacteria. Microbiol. Rev. **57:**543–594.
25. **Pridmore, R. D., B. Berger, F. Desiere, D. Vilanova, C. Barretto, A.-C. Pittet, M.-C. Zwahlen, M. Rouvet, E. Altermann, R. Barrangou, B. Mollet, A. Mercenier, T. Klaenhammer, F. Arigoni, and M. A. Schell.** 2004. The genome sequence of the probiotic intestinal bacterium *Lactobacillus johnsonii* NCC 533. Proc. Natl. Acad. Sci. USA **101:**2512–2517.
26. **Raasch, C., M. Armbrecht, W. Streit, B. Höcker, N. Sträter, and W. Liebl.** 2002. Identification of residues important for NAD^+ binding by the *Thermotoga maritima* α-glucosidase AglA, a member of the glycoside hydrolase family 4. FEBS Lett. **517:**267–271.
27. **Raasch, C., W. Streit, J. Schanzer, M. Bibel, U. Gosslar, and W. Liebl.** 2000. *Thermotoga maritima* AglA, an extremely thermostable NAD^+-, Mn^{2+}-, and thiol-dependent α-glucosidase. Extremophiles **4:**189–200.
28. **Rajan, S. S., X. Yang, F. Collart, V. L. Y. Yip, S. G. Withers, A. Varrot, J. Thompson, G. J. Davies, and W. F. Anderson.** 2004. Novel catalytic mechanism of glycoside hydrolysis based on the structure of an NAD^+/Mn^{2+}-dependent phospho-α-glucosidase from *Bacillus subtilis*. Structure **12:**1619–1629.
29. **Reizer, J., M. H. Saier, Jr., J. Deutscher, F. Grenier, J. Thompson, and W. Hengstenberg.** 1988. The phosphoenolpyruvate:sugar phosphotransferase system in gram-positive bacteria: properties, mechanism, and regulation. Crit. Rev. Microbiol. **15:**297–338.
30. **Robrish, S. A., H. M. Fales, C. Gentry-Weeks, and J. Thompson.** 1994. Phosphoenolpyruvate-dependent maltose: phosphotransferase activity in *Fusobacterium mortiferum* ATCC 25557: specificity, inducibility, and product analysis. J. Bacteriol. **176:**3250–3256.
31. **Rye, C. S., and S. G. Withers.** 2000. Glycosidase mechanisms. Curr. Opin. Chem. Biol. **4:**573–580.
32. **Sambrook, J., E. F. Fritsch, and T. Maniatis.** 1989. Molecular cloning: a laboratory manual, 2nd ed. Cold Spring Harbor Laboratory Press, Cold Spring Harbor, NY.
33. **Thompson, J., C. R. Gentry-Weeks, N. Y. Nguyen, J. E. Folk, and S. A. Robrish.** 1995. Purification from *Fusobacterium mortiferum* ATCC 25557 of a 6-phosphoryl-*O*-α-D-glucopyranosyl:6-phosphoglucohydrolase that hydrolyzes maltose 6-phosphate and related phospho-α-D-glucosides. J. Bacteriol. **177:**2505–2512.
34. **Thompson, J., S. Hess, and A. Pikis.** 2004. Genes *malH* and *pagl* of *Clostridium acetobutylicum* ATCC 824 encode NAD^+- and Mn^{2+}-dependent phospho-α-glucosidase(s). J. Biol. Chem. **279:**1553–1561.
35. **Thompson, J., F. W. Lichtenthaler, S. Peters, and A. Pikis.** 2002. β-Glu-

coside kinase (BglK) from *Klebsiella pneumoniae*: purification, properties, and synthesis of 6-phospho-β-D-glucosides. J. Biol. Chem. **277:**34310–34321.
36. **Thompson, J., A. Pikis, S. B. Ruvinov, B. Henrissat, H. Yamamoto, and J. Sekiguchi.** 1998. The gene *glvA* of *Bacillus subtilis* 168 encodes a metal-requiring, NAD(H)-dependent 6-phospho-α-glucosidase. J. Biol. Chem. **273:** 27347–27356.
37. **Thompson, J., S. A. Robrish, S. Immel, F. W. Lichtenthaler, B. G. Hall, and A. Pikis.** 2001. Metabolism of sucrose and its five linkage-isomeric α-D-glucosyl-D-fructoses by *Klebsiella pneumoniae*: participation and properties of sucrose-6-phosphate hydrolase and phospho-α-glucosidase. J. Biol. Chem. **276:**37415–37425.
38. **Thompson, J., S. A. Robrish, A. Pikis, A. Brust, and F. W. Lichtenthaler.** 2001. Phosphorylation and metabolism of sucrose and its five linkage-isomeric α-D-glucosyl-D-fructoses by *Klebsiella pneumoniae*. Carbohydr. Res. **331:**149–161.
39. **Thompson, J., S. B. Ruvinov, D. I. Freedberg, and B. G. Hall.** 1999. Cellobiose-6-phosphate hydrolase (CelF) of *Escherichia coli*: characterization and assignment to the unusual family 4 of glycosylhydrolases. J. Bacteriol. **181:** 7339–7345.
40. **Varrot, A., V. L. Y. Yip, Y. Li, S. S. Rajan, X. Yang, W. F. Anderson, J. Thompson, S. G. Withers, and G. J. Davies.** 2005. NAD^+ and metal-ion dependent hydrolysis by family 4 glycosidases: structural insight into specificity for phospho-β-glucosides. J. Mol. Biol. **346:**423–435.
41. **Veyrat, A., V. Monedero, and G. Pérez-Martinez.** 1994. Glucose transport by the phosphoenolpyruvate:mannose phosphotransferase system in *Lactobacillus casei* ATCC 393 and its role in carbon catabolite repression. Microbiology **140:**1141–1149.
42. **Viana, R., V. Monedero, V. Dossonnet, C. Vadeboncoeur, G. Pérez-Martínez, and J. Deutscher.** 2000. Enzyme I and HPr from *Lactobacillus casei*: their role in sugar transport, carbon catabolite repression and inducer exclusion. Mol. Microbiol. **36:**570–584.
43. **Wilson, G., and C. F. Fox.** 1974. The β-glucoside system of *Escherichia coli*. IV. Purification and properties of phospho-β-glucosidases A and B. J. Biol. Chem. **249:**5586–5598.
44. **Witt, E., R. Frank, and W. Hengstenberg.** 1993. 6-Phospho-β-galactosidases of Gram-positive and 6-phospho-β-glucosidase B of Gram-negative bacteria: comparison of structure and function by kinetic and immunological methods and mutagenesis of the *lacG* gene of *Staphylococcus aureus*. Protein Eng. **6:**913–929.
45. **Yebra, M. J., V. Monedero, M. Zuniga, J. Deutscher, and G. Pérez-Martínez.** 2006. Molecular analysis of the glucose-specific phosphoenolpyruvate:sugar phosphotransferase system from *Lactobacillus casei* and its links with the control of sugar metabolism. Microbiology **152:**95–104.
46. **Yebra, M. J., A. Veyrat, M. A. Santos, and G. Pérez-Martínez.** 2000. Genetics of L-sorbose transport and metabolism in *Lactobacillus casei*. J. Bacteriol. **182:**155–163.
47. **Yip, V. L. Y., J. Thompson, and S. G. Withers.** 2007. Mechanism of GlvA from *Bacillus subtilis*: a detailed kinetic analysis of a 6-phospho-α-glucosidase from glycoside hydrolase family 4. Biochemistry **46:**9840–9852.
48. **Yip, V. L. Y., A. Varrot, G. J. Davies, S. S. Rajan, X. Yang, J. Thompson, W. F. Anderson, and S. G. Withers.** 2004. An unusual mechanism of glycoside hydrolysis involving redox and elimination steps by a family 4 β-glycosidase from *Thermotoga maritima*. J. Am. Chem. Soc. **126:**8354–8355.
49. **Yip, V. L. Y., and S. G. Withers.** 2006. Family 4 glycoside hydrolases are special: the first β-elimination mechanism amongst glycoside hydrolases. Biocatal. Biotransform. **24:**167–176.
50. **Zechel, D. L., and S. G. Withers.** 2000. Glycosidase mechanisms: anatomy of a finely tuned catalyst. Acc. Chem. Res. **33:**11–18.
51. **Zechel, D. L., and S. G. Withers.** 2001. Dissection of nucleophilic and acid-base catalysis in glycosidases. Curr. Opin. Chem. Biol. **5:**643–649.